

## Some Alignment Concepts for the GEM Muon Array

J. Paradiso  
C.S. Draper Laboratory

June 1992

### Abstract:

This report introduces a basic alignment scheme for the GEM muon detector. Optical straightness monitors are described, and their application discussed. Alternative alignment technologies are suggested and techniques are identified that can provide multipoint measurements. The problem of global alignment is posed, and several concepts are presented to attain the required precision.

# Some Alignment Concepts for the GEM Muon Array

-- J. Paradiso, June '92

Each phi sector of the muon detector array (i.e. "hexant") will be instrumented to monitor the relative alignment of its composite drift chamber layers. The most critical such measurement is the deviation in chamber alignment from a straight line along a muon path. If the 3 superlayers are relatively displaced along the muon bending direction, a false sagitta will result, leading to errors in the momentum measurement. In order to retain the quoted 5-10% momentum resolution of the GEM muon detector, the allowed misalignment of sense wires between chamber superlayers must be limited to  $\pm 25 \mu\text{m}$  (in the bending coordinate).

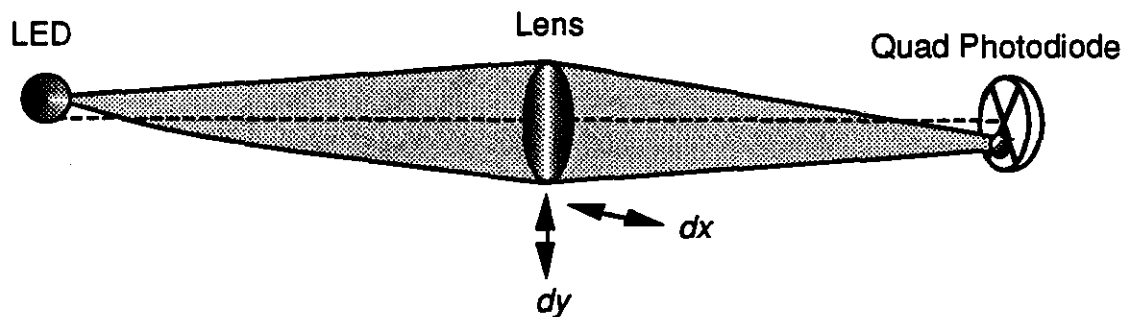


Figure 1: The Basic Straightness Monitor

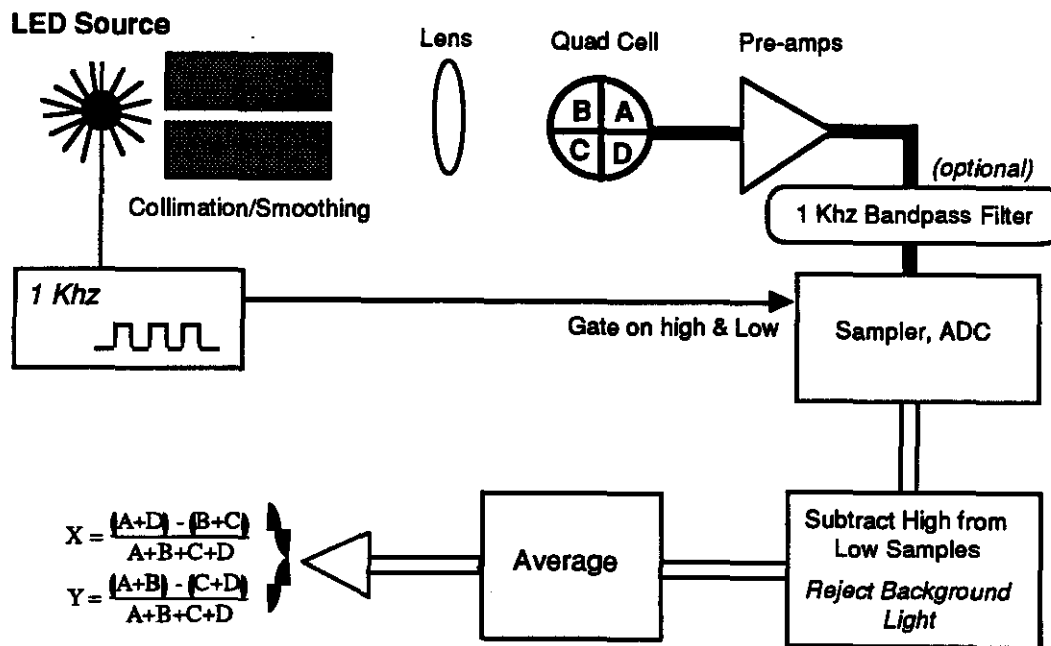


Figure 2: Straightness Monitor Electronics

Linear range can be extended by defocusing:  
Comparison 0, .4, 10, 20 cm defocus (LED 1102, ambient light on)

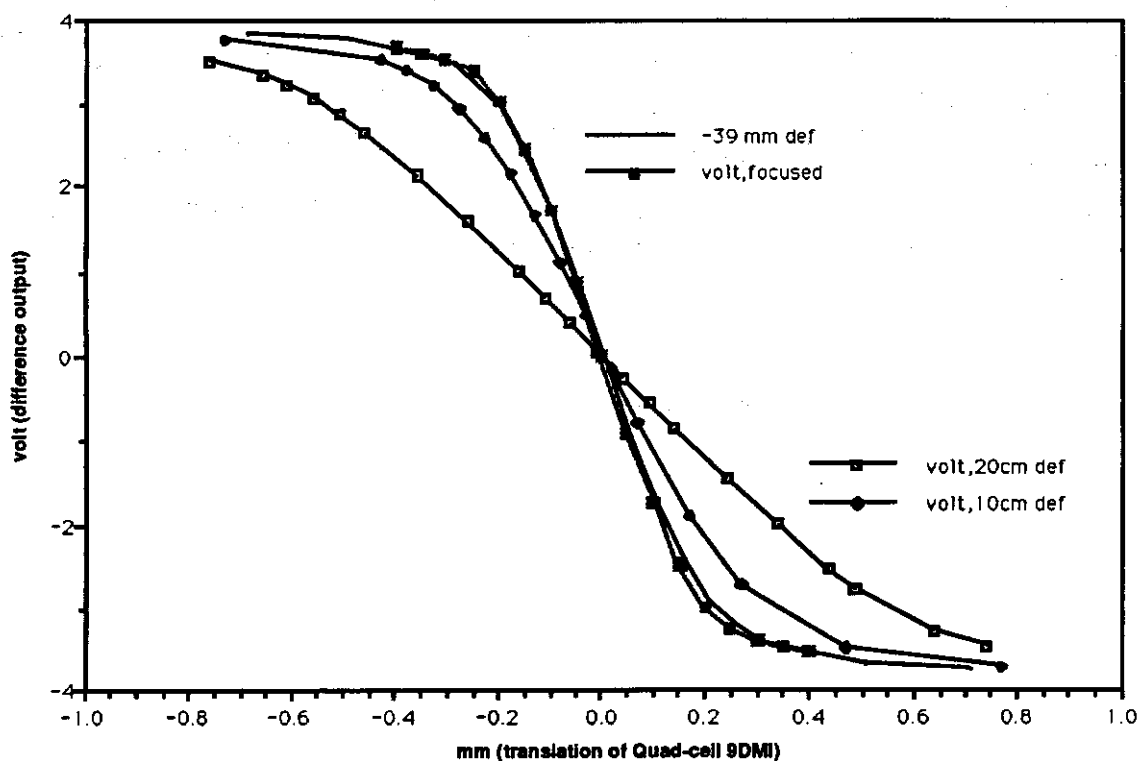


Figure 3: Straightness Monitor Transfer Function

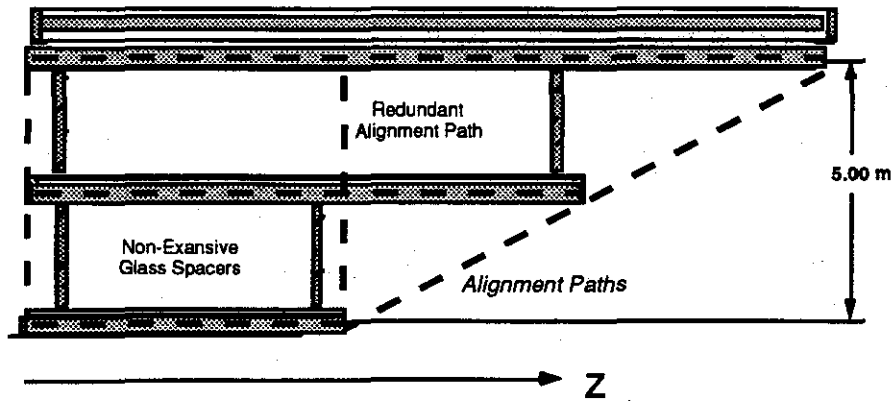
This quantity can be measured by optical instruments based on the "straightness monitors"<sup>1</sup> that were successfully used in the L3 experiment<sup>2</sup>. These are simple devices composed of an LED, lens, and quadrant photodiode, as shown in Fig. 1. An image of a smooth-aperture, collimated source (i.e. LED) is projected onto a planar detector (i.e. quadrant photodiode) through a focusing lens. Displacements of the lens from the line between source and detector are detected by a shift in the illumination centroid at the photodiode. The measured displacement is insensitive to rotations of the components about their optical axes. The LED is modulated by a low-frequency square wave, and synchronously detected to minimize the effects of any ambient light background, as shown in Fig. 2. The straightness monitor components will be fixed to the drift chamber packages such that they precisely reference the sense wire positions. The mounts containing the optical devices and the gain balance between detector quadrants will be precisely adjusted as these components are fabricated. During construction of each muon segment, the straightness monitors will be cross-checked using cosmic ray data and external measurements.

Straightness monitor systems are known to be capable of extremely high resolution (i.e. under  $2\text{ }\mu\text{m}$  is commonly achieved<sup>3</sup>), but their practical accuracy is limited by systematic errors, contributed primarily through the mechanics that mount the components. The 6 micron net precision quoted for the L3 monitors<sup>4</sup> is adopted as a baseline accuracy for the GEM straightness system. Since some of the optical path lengths needed for the GEM system can be significantly longer than at L3 (particularly at the endcaps), the effects of thermal gradients and atmospheric disturbances must be ascertained. Recent tests have retained high straightness monitor accuracy over a 9 meter path<sup>5</sup>. Path lengths will be extended by integrating over many samples and randomizing the thermal gradients by maintaining a steady airflow. These devices are quite inexpensive; installed straightness monitor systems have recently been estimated<sup>5</sup> to cost roughly \$500. per 3-point string.

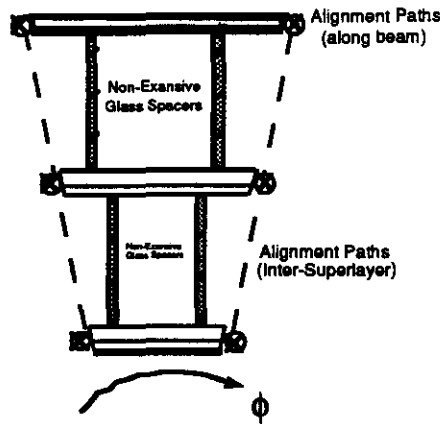
The dynamic range of these devices can be quite limited; i.e. the monitors used at L3 have a useful measurement range of roughly  $200\text{ }\mu\text{m}$ . Test data from a straightness monitor setup<sup>5</sup> is shown in Fig. 3; the dynamic range for the largest spot (most defocused) approaches 1 mm. Nonhomogeneity of the light spot can affect the linearity of calibration curves; the measurements shown in Fig. 3 employ a special IR LED that incorporates an integral glass ball diffuser lens to smooth the illumination function. By imaging a square rather than a circle, and expanding the image size to occupy more of the diode surface, a wider range can be obtained (ultimately up to several mm).

The range can be also extended by employing different types of detectors that are capable of operating in the magnetic field, such as lateral-effect photodiodes or "photopots", which spatially weight the sensitivity of the quadrants, and imagers like CCDs<sup>6</sup> or photodiode arrays [which are now packaged as devices that intrinsically output an illumination centroid over a wide range; i.e. Ref. 7]. Research in this area is currently proceeding, with the goal of achieving a measurement range above 2 mm; ideally, it should be possible to span a precision measurement across a range of  $\pm 5\text{ mm}$ .

The proposed implementation of the straightness monitors is given in Fig. 4, where alignment paths are denoted by dashed lines. Multipoint straightness monitors will be directed along the chamber packages in the z direction. These will be mounted at points that reference the sense wires in a chamber layer (i.e. at positions where the wires are supported, or between chamber package boundaries), and will insure the straightness of wires in each chamber layer. They may be implemented by leapfrogging several sets of standard 3-point monitors (Fig. 5a), or by employing a multipoint alignment scheme, such as provided by the stretched wire alignment technique (SWAT), which has been used to align components to the micron level over large distances<sup>8,9</sup>. To apply the latter



a)  $r\theta$  View



b)  $r\phi$  View

**Figure 4: Straightness Monitor Paths in Muon Chamber Barrel**

method, a narrow wire will be stretched between the superlayer endpoints in  $z$ , and its displacement measured at the locations of the drift chamber wire supports (Fig. 5b). The wire position will be determined relative to the chamber fiducials by an inexpensive optical means (i.e. encapsulated proximity sensors<sup>8</sup>, which have been shown to yield a dynamic range of roughly 1 mm; see Fig. 6), or capacitive techniques<sup>9</sup>. By regulating the tension to a known value, the wire sag can be determined and the measurements compensated. In order to reduce sensitivity to structural and atmospheric dynamics, the wire will be stretched to sufficient tension and protected in a tube.

Several optical multipoint alignment schemes (i.e. see Ref. 10) are currently being developed that have intrinsic simplicity and potential reliability advantages over a wire technique. One elegant solution<sup>11</sup> is to use multistrip silicon detectors (making a wafer of about 50 micron thickness, 1-2 cm length, 300  $\mu\text{m}$  strip pitch) to detect the centroid of

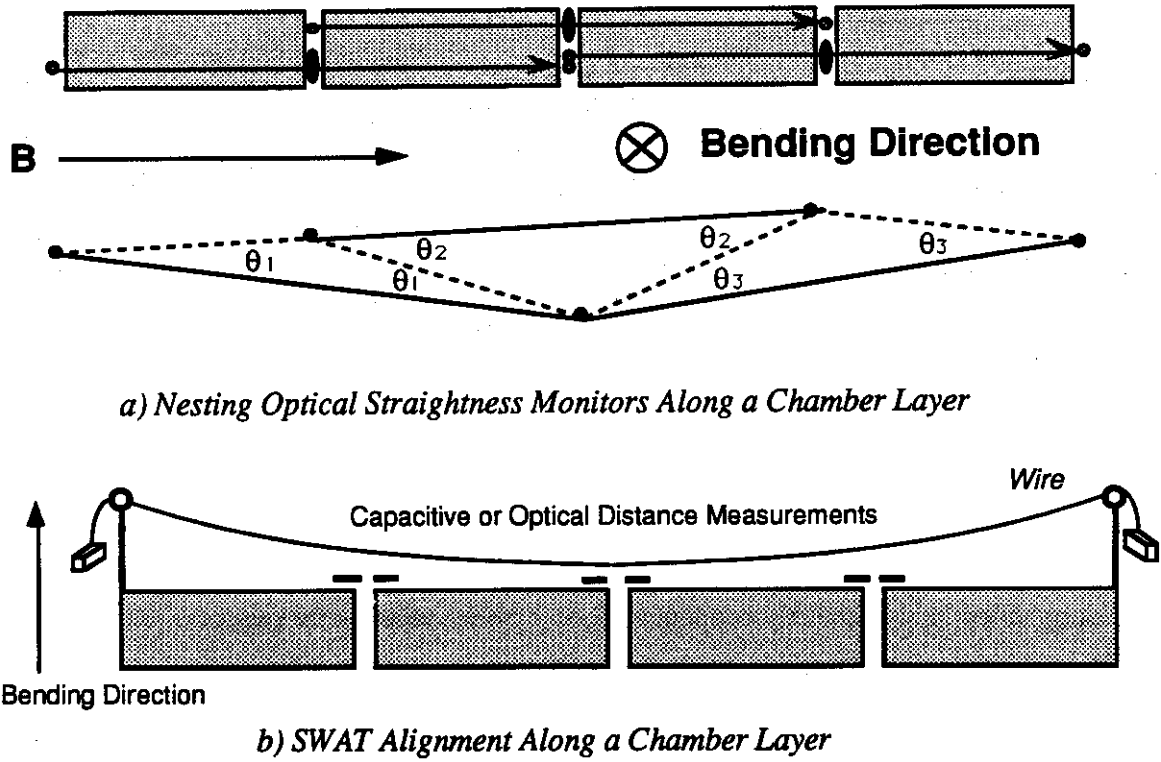
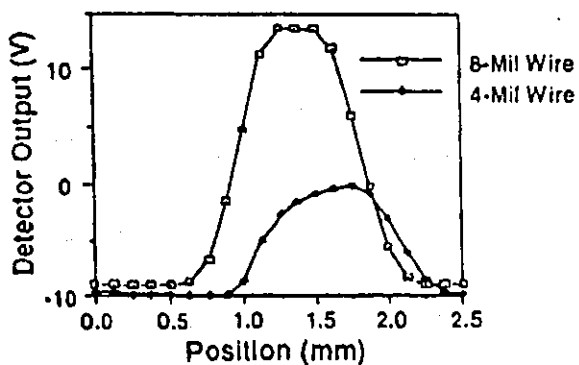


**Figure 5: Multipoint Alignment along Beam Axis**

illumination of an IR laser that emits at a wavelength (i.e.  $1.06 \mu\text{m}$ ) where the silicon wafers are better than 90% transparent. These wafers can then be stacked along the beam, and the beam centroid determined (at the micron level) as projected onto each wafer. Such devices are in initial development; potential difficulties involving fabrication, optical properties (i.e. refraction through the wafer), dust accumulation, and design/cost of readout electronics (i.e. up to 70 preamplifier channels needed per wafer) must be resolved before these techniques can be baselined into the GEM muon array.

The alignment paths that relate different chamber layers are also shown as dashed lines in Fig. 4a. The vertical line at left and angled line at right are needed, as they provide references along the muon path. The vertical line at the center of Fig. 4a represents a redundant alignment path, which will present a useful cross-check (unlike the depiction of Fig. 4a, this path is best implemented as another projective line pointing to the IP; although schemes with 3 or more projective alignment paths are currently under consideration, the loss in  $\theta$  acceptance may be prohibitively large, particularly at the inner chamber layer).



The photodetectors used to measure wire deflections are very sensitive---the output for a 4-mil wire is greater than 20 millivolts per micron of motion!

Figure 6: Measured transfer function of SWAT alignment system (from Ref. 8)

Alignment fixtures are installed at points where the chamber sense wires or pickup strips can be directly referenced (i.e. at points where wire supports [for the limited streamer drift tube option] or drift-tube bulkheads [pressurized drift tubes] are located, or directly on the cathode planes [for cathode strip chambers]). In order to interrelate chamber layers through the straightness monitor scheme of Fig. 4, these fixtures must line up between superlayers, preferably in a projective fashion. Other alignment measuring techniques could relax this requirement; i.e. a "laser beacon" <sup>10,12</sup> can be used to define a plane of illumination, which can then be referenced at various points along the side of a hexant (i.e. distance from the chamber fiducial to the beacon plane defines the sagitta error). Laser beacons require significant mechanical precision (i.e. the rotor must create a plane accurate to  $5 \mu\text{rad}$ <sup>13</sup>), and function in a magnetic field, which has inspired difficulties with similar devices at L3. In addition, sufficient space must be allocated along the edge of the chamber arrays to support the rotor assembly, and optical paths must be guaranteed between the rotor and all sensors. While the laser beacon concept does meet some of the conceptual alignment needs, it will require significant engineering development before becoming a strong alternative.

These alignment paths (i.e. multipoint alignment along a layer, and interlayer alignments) will be instrumented along each side of a muon hexant, as depicted in Fig. 4b. Employing the straightness monitors of Fig. 1 will require lens diameters on the order of 1" (for the 90° path) and 2" (for the 30° path) to ensure sufficient light collection from the LED (a stronger source, such as a spatially stable diode laser, could reduce this diameter, although appreciably increasing the overall expense). The radial displacements of chamber layers (orthogonal to the bending direction) will also couple into the bending measurement at the edges of the hexants in Fig. 4b, producing a needed radial spacing

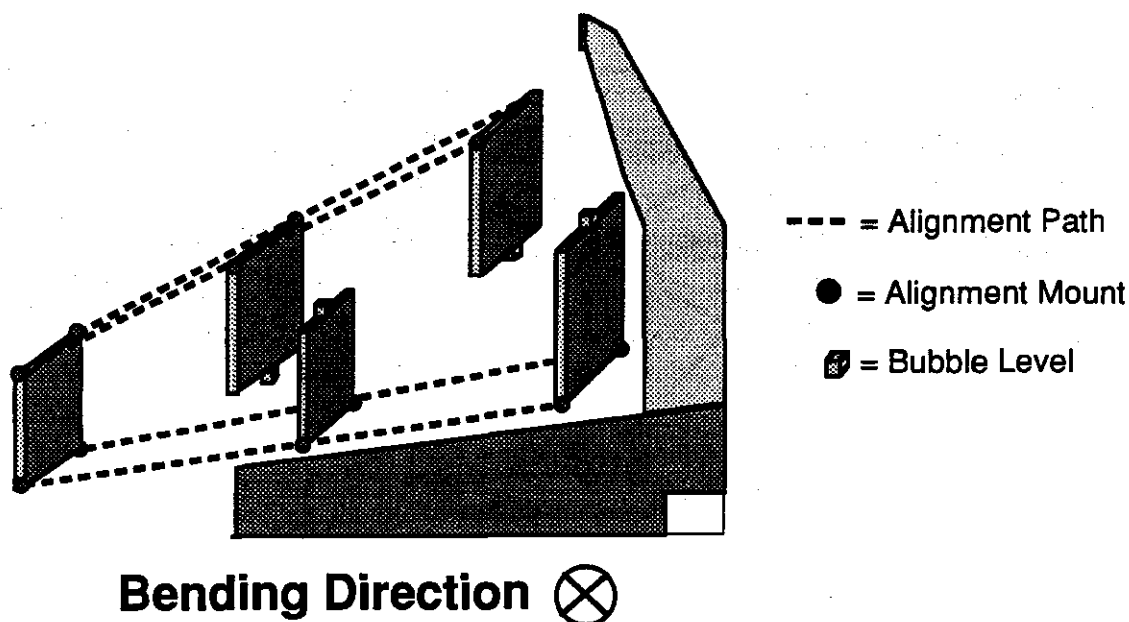


**Figure 7: Alignment Paths in the Muon Endcaps**

accuracy of  $60 \mu\text{m}^{14}$ . Since this is also monitored by the alignment paths directed along the hexant sides, an explicit measurement of the radial layer displacement may not be required; if needed, a precision rod equipped with a range measurement (i.e. capacitive sensor or mechanical gauge) will determine this shift with sufficient accuracy, as shown in Fig. 4 (this measurement will be translated across the multiple chamber packages in a superlayer by the multipoint monitors outlined in Fig. 5). While alignment along the beam (z) axis is not critical, it will nonetheless be precisely measured via the straightness monitor systems, which are sensitive in two coordinates.

The L3 experiment also employed a rotating laser beacon system<sup>12</sup> to determine the coplanarity of the straightness monitor lines, and thus measure the torque in the hexant structure. Since straightness monitors will be directed along the muon paths at maximum and minimum  $\theta$  (Fig. 4a), and will be installed on both sides of the hexant (Fig. 4b), a "torque" angle (about the z-axis) between alignment lines-of-sight will not create a sagitta error<sup>14</sup>, hence the additional planarity measurement is unnecessary.

Alignment paths will be defined at the maximum and minimum  $\theta$  spanned by the endcap array, as portrayed in Fig. 7. The dashed lines shown in Fig. 7 show a pair alignment paths, one near each  $\phi$  extreme covered by an endcap "hexant" module. These insure that the chamber layers are not twisted in  $\phi$ , which can create an error in the momentum measurement. The alignment mounts will be fixed to precisely defined points



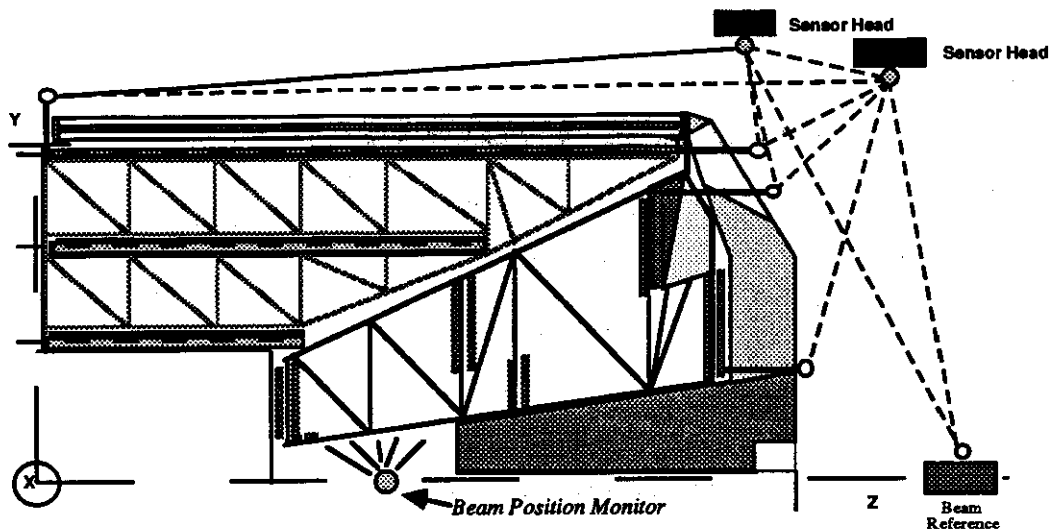


Figure 8: Strategies for Measuring Global Muon System Alignment

on the cathode plane and Hexcell laminate, which will provide a stable reference to the spacepoint measurements. If needed, a measurement of the differential torque between upper and lower chamber layer components (middle, outer layers) can be determined by using bubble levels, of the sort employed in the L3 octant tests<sup>1</sup>. If required, measurements of chamber offsets in the  $z$  direction (which couple into the momentum measurement, and must be determined to within  $125 \mu\text{m}^{14}$ ) can be made with simple mechanical techniques, as suggested for determining the radial chamber spacing in the barrel, or with optical range measuring systems (again, since the alignment lines are projective to the IP, the sagitta error introduced through radial displacement will be detected by the straightness monitors).

Several aspects of the endcap chamber layout are simplified in Fig. 7. In particular, the endcap superlayers are split into several packages displaced along  $z$ . This is especially relevant at small  $\theta$ , where small chambers abound to handle the large rate & occupancy expected at high  $\eta$ . The scheme of Fig. 7 assumes that the superlayer chambers will all be referenced to the straightness monitor fixture, either by precision mechanics or by another (short-range) alignment system. Since the required accuracy is so high here (i.e. the alignment transfer between fixture and chambers should be well below  $50 \mu\text{m}$ , as discussed below), achieving this common alignment reference may not be trivial. A potential alternative here may be to employ a multipoint alignment scheme (i.e. a wire-based "SWAT" technique or a multipoint optical method) to pick a reference off each chamber independently, rather than take a single alignment reading relative to the center of a poorly linked superlayer. Clearly, more detail needs to be established here as the endcap design evolves.

The position of the muon detector components must be determined relative to the interaction region. This will be attempted by tracking muons through the entire detector, thereby tying the muon array to the central tracker (which will find its own reference to the beamline). An independent check of global muon system alignment, however, will aid in reducing systematic error sources. Although a 200  $\mu\text{m}$  precision would be ultimately desired in the  $r\phi$  plane for enhanced momentum resolution, an alignment on the millimeter scale will be adequate for most physics goals. Muon events themselves may be sufficient to determine this alignment on-line, provided that enough high-momentum muons will be produced over the full acceptance in  $\eta$  to statistically link the central tracker coordinates to those of the muon array; otherwise a set of automatic survey techniques can monitor the detector position, as depicted in Fig. 8 and discussed below.

A promising method of aligning to the beamline requires placing a pair of beam position monitors inside the detector (on each side, between the calorimeter endcaps and flux concentrators) to dynamically measure the beam location. One can then measure the distance between a point referenced to the beam position monitors and the several positions on the muon array. Since the distances are relatively short, and lines of sight will be readily available to a large portion of the muon array, achieving the required 200  $\mu\text{m}$  accuracy should be possible through a variety of techniques (i.e. optical range/angle, mechanical displacement measurements with thermally invariant rods and/or stress-free structures, etc.). The feasibility of this approach is currently under investigation.

An alternative approach to attaining global muon system alignment is to sight out through holes in the flux concentrator support (and, if possible, through the central membrane gap), to sensors at various reference points in the hall. These sensors, which can be placed in known positions relative to the beamline, can measure the range to several points on the muon detector. The range measurements can be performed by detecting the returned phase of an AM signal modulated onto an optical carrier (as used in commercial surveying equipment<sup>15</sup>). The range measurement is much less sensitive to atmospheric disturbance than an angular measurement; by making many redundant measurements and monitoring the temperature in the hall, it should be possible to achieve the required resolution, although certainly at some expense.

If the dynamic forces on the muon array (mainly due to the shift in shape of the containment vessel as the magnet is powered on and off) are kept small, the change in orientation of the muon hexants can be measured around the vertical with an inexpensive instrumented level system. Together with a model of the structural response, the change in hexant position and orientation may be determined from these measurements, and the initial survey model updated accordingly.

Global alignment for the muon system can be interpreted as the need to direct the radial straightness monitor axes toward the interaction point (as in the scheme depicted by Fig. 4). Optical multipoint alignment techniques that are able to extend the alignment path to the outside of the detector (potentially feasible for the vertical lines near the magnet membrane and the horizontal lines along the z axis; more difficult for the 30° line) may be well suited to determining the global detector alignment. A practical design that incorporates such an approach, however, remains to be determined.

In summary, the precision required by the muon alignment systems is given below (as adapted from Ref. 14, where these figures are presented in more detail): In both the muon barrel and endcaps, the " $\phi$ " coordinate refers to the bending direction, referenced at the center of each hexant. The "r" coordinate refers to the radial distance from the beamline, and the "z" coordinate is defined to be the beam direction (referenced to the IP). The local alignment ("between superlayers") is assumed to be referenced to the mean position of the composite chambers (the chambers themselves are allowed to have a 50  $\mu\text{m}$  alignment scatter (in  $\phi$ ), provided that the superlayer reference is taken at the mean).

<i>Local Alignment (between superlayers)</i>	<i>Global Alignment (to IP)</i>
<b>Muon Barrel</b>	
Bending Coordinate ( $\phi$ ): 25 $\mu\text{m}$	$\phi$ : 5 mm (200 $\mu\text{m}$ goal)
Radial Coordinate (r): 60 $\mu\text{m}$	r: 10 mm
Beamline Coordinate (z): 1 mm	z: 5 mm
<b>Muon Endcaps</b>	
Bending Coordinate ( $\phi$ ): 25 $\mu\text{m}$	$\phi$ : 5 mm (200 $\mu\text{m}$ goal)
Radial Coordinate (r): 1 mm	r: 4 mm
Beamline Coordinate (z): 125 $\mu\text{m}$	z: 10 mm

## References

- 1) Toth, W. E., "Muon Detector Program; Prototype Octant Construction and Evaluation with Production Phase Recommendations", Draper Lab Report CSDL-R-1885, Oct. 1987.
- 2) Adeva, B. et. al., "The Construction of the L3 Experiment", *Nuc. Inst. and Methods*, A289 (1990), pg. 35.
- 3) VanderGraff, H., NIKHEF Amsterdam, Personal communication, March, 1992.
- 4) Duinker, P., et. al., "Some Methods for Testing and Optimizing Proportional Wire Chambers", *Nuc. Inst. and Methods*, A273 (1988), pg. 814-819.
- 5) Ayer, F. et. al., "The Engineering Development of an Actively Controlled Precise Muon Chamber for the SDC Detector", *Proc. of the SSCIII Conference, New Orleans, LA*, March 1992.
- 6) Becker, U. and Paradiso, J., "An Optical CCD-based System for Precise Drift Chamber Positioning", *Nuc. Inst. and Methods*, 196, p. 381 (1982).
- 7) See devices such as the "MULTISCAN" Position-sensitive photodetector (from Technoexan, c/o Semicon Inc., Ontario, Canada), also J. Wyatt et. al., results from the MIT Lincoln Lab vision project.
- 8) Griffith, L., LLNL, Presentation at GEM Alignment Meeting, SSCL, May 22, 1992.
- 9) Coosemans, W., Lasseur, C., CERN, Geneva, Personal communication, June 9, 1992.
- 10) Sawicki, R., LLNL, "Muon Chamber Alignment Alternatives", Presentation at SSCL alignment meeting, June 12, 1992.
- 11) Blum, W., Max Plank Institute, Presentation on silicon multistrip detectors for multipoint alignment, SSCL, June 17, 1992.
- 12) Seiler, P.G., et al., "The Laser Beacon", L3 Muon Chamber Group Internal Note, 85-4, 1985.

- 13) Zhukov, V., GEM muon alignment requirements summary, June, 1992.
- 14) Paradiso, J. "Alignment Requirements for the GEM Muon Detector", June, 1992.
- 15) Rueger, J.M., Electronic Distance Measurement, Third Edition, Springer-Verlag, 1990.